Bioconjugate Chemistry

Article

pubs.acs.org/bc

Functionalization of the PEG Corona of Nanoparticles by Clip Photochemistry in Water: Application to the Grafting of RGD Ligands on PEGylated USPIO Imaging Agent

Vincent Pourcelle,[‡] Sophie Laurent,[§,#] Alexandre Welle,[‡] Nicolas Vriamont,[‡] Dimitri Stanicki,[§] Luce Vander Elst,[§,#] Robert N. Muller,[§,#] and Jacqueline Marchand-Brynaert*[,‡]

[‡]Institute of Condensed Matter and Nanosciences, Université catholique de Louvain, Place Louis Pasteur 1 bte L4.01.02, 1348 Louvain-La-Neuve, Belgium

[§]Department of General, Organic and Biomedical Chemistry, NMR and Molecular Imaging Laboratory, University of Mons, B-7000 Mons, Belgium

[#]Center for Microscopy and Molecular Imaging (CMMI), Rue Adrienne Bolland, 8 B-6041 Gosselies, Belgium

Supporting Information

ABSTRACT: The fast development of nanomedicines requires more and more reliable chemical tools in order to accurately design materials and control the surface properties of the nano-objects used in biomedical applications. In this study we describe a smooth and simple photografting technique, i.e., the clip photochemistry, that allows the introduction of molecules of interest in inert polymers or on stealth nanoparticles directly in aqueous solution. First we developed the methodology on polyethylene glycol (PEG) and looked for critical parameters of the process (irradiation times, concentrations, washings) by using several molecular probes and adapted analytical techniques (^{19}F qNMR, EA, LSC). We found that the clip photochemistry in water is a robust and efficient method to functionalize PEG. Second we applied it on PEGylated USPIO (USPIO-PEG) magnetic resonance imaging agent and succeeded in introducing RGD peptide and homemade peptidomimetics on their PEG segments. The magnetic abilities of the conjugated nanoparticles were unchanged by the derivatization process as evidenced by their relaxometric properties and their NMRD profile. When tested on Jurkat lymphocyte T Cells, which express $\alpha_v\beta_3$ integrins, the USPIO conjugated with RGD ligands leads to an increase of the transverse relaxation rate (R_2) by a factor 10 to 14 as compared to USPIO-PEG. Consequently, it makes them good candidates for targeted imaging technology in cancer therapy.

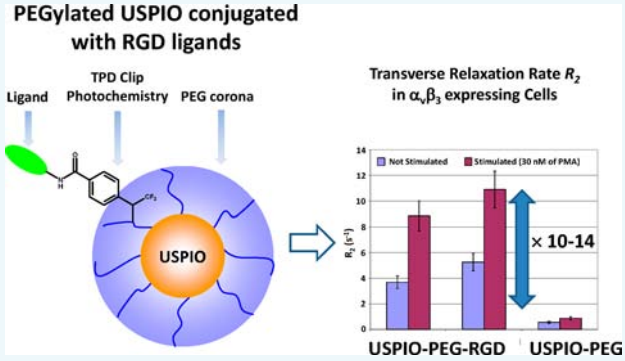

INTRODUCTION

In the scope of the development of nanomedicines, the realization of multifunctional nanoparticles (e.g., targeted drug delivery system with imaging or diagnosis abilities) has increased in complexity and has become a real challenge. At the same time, recent critical reviews have pointed out that the lack of translation of promising nanotherapies, from the bench to the bed side, may be due to irrelevant methods of preparation.[1−5] In this context there is a need for new chemical tools.

Over several years we have developed a smooth and versatile "clip photochemistry" technique in order to introduce reactive *N*-hydroxysuccinimidyl (NHS) ester along a polymer chain.[6,7] The principle is to take advantage of bireactive linkers which own a light activatable function (i.e., 3-phenyl-3-(trifluoromethyl) diazirine (TPD)[8] or perfluorophenyl azide (PFPA)[9]) on one side and a NHS ester on the other side. This is a straightforward way to functionalize inert commercial substrates that avoid the tricky elaboration of reactive materials.[10−14] Due to the presence of very reactive intermediates, the process is mostly practiced under inert atmosphere, on clean surfaces or in the bulk of pure soft materials. The literature presents very few examples of this photografting method in liquid media. Beside the photoaffinity labeling (PAL) of biological targets,[15,16] the direct photochemical functionalization of polymers (PEGs) in solution has been described, with moderate success.[17,18]

One way to avoid a loss of reactivity in the liquid phase is to design orthogonal photoconjugation processes based on the recent development of the "photo-click reactions". Barner-Kowollik's group has done pioneering work in this domain with phototriggered Diels−Alder reactions[19] or nitrile imine-mediated tetrazole-ene cycloadditions (NITEC).[20] Popik's group developed very fast and straightforward Diels−Alder or

Received: January 19, 2015
Revised: April 6, 2015
Published: April 8, 2015

DOI: 10.1021/acs.bioconjchem.5b00041
Bioconjugate Chem. 2015, 26, 822−829

Scheme 1. "Clip Photochemistry" to Obtain NHS Functionalized PEG Followed by Chemical Derivatization with Molecular Probes

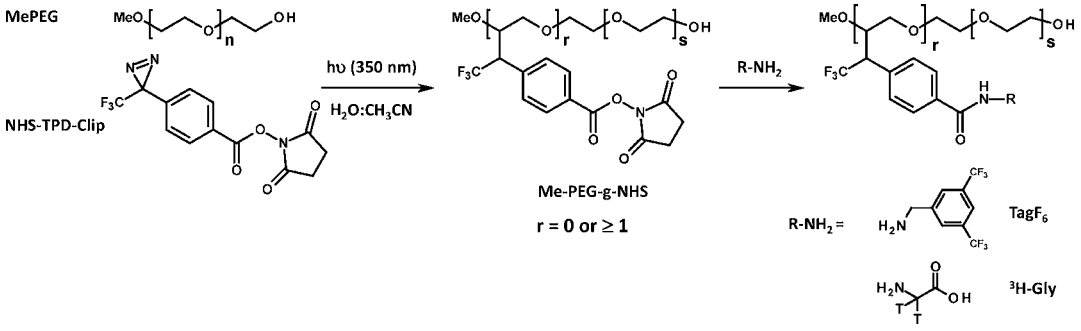

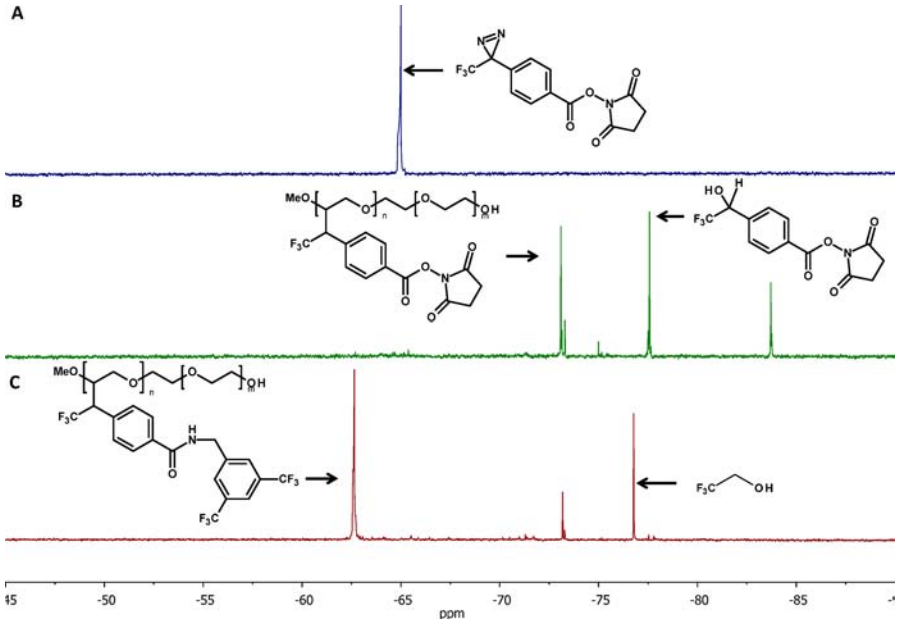

Figure 1. Stacked ^{19}F NMR (282.09 MHz, D_2O:CD_3CN) spectra of the PEG clip photochemistry process and derivatization with $TagF_6$ under condition A ([PEG_{2k}] = 20 mM, [TDP clip] = 10 mM); (A) PEG mixed with NHS-TPD clip before irradiation; (B) crude PEG-*g*-NHS obtained after 30 min of irradiation at 350 nm; (C) purified PEG-clip-$TagF_6$ with trifluoroethanol as internal standard for ^{19}F qNMR.

strain-promoted azide−alkyne cycloaddition (SPAAC) initiated under UV activation.[21,22] Both approaches are not straightforward and require first a multistep chemical derivatization of the substrates in order to have the desired functions to fulfill whether a Diels−Alder or a 1,3-dipolar cycloaddition.

In precedent studies concerning nanomedicines, we introduced the targeting ligands on dry materials prior to their formulation as a biomedical device.[13,23,24] This method raises the question, where will the targeting moieties be located: displayed on the external corona or hindered in the inside layers? Indeed, the control of the situation of the targeting ligands after self-assembling is a difficult but crucial question.[25] For instance, it was observed that a lipophilic ligand at the distal end of a PLGA−PEG copolymer ended in the core of nanoparticles after self-assembly.[26] We see, with the photografting in aqueous solution, an easy way to anchor ligands exclusively on the external soluble parts of particles. Moreover, complex systems that cannot be dried, such as nanoparticles in colloidal suspension, might be ideally treated in water.

Previously, we have grafted a Gly-Arg-Gly-Asp-Ser (GRGDS named RGD) peptide and a synthetic RGD peptidomimetic (RGDp) on ultrasmall iron oxide particles (USPIO) used as magnetic resonance imaging (MRI) contrast agents.[27,28] RGD and analogues target integrin $\alpha_v\beta_3$ which is a membrane receptor overexpressed by cancer cells and angiogenic endothelium. It was also evidenced that the targeting of this receptor enhanced the cellular uptake of particles.[29] We succeeded in introducing the RGDs on freeze-dried USPIO, but with low yields and significant aggregation and material losses. Anyway, the targeted USPIO showed unchanged magnetic properties and enhanced in vitro labeling efficiency as compared to the native particles.[27] Targeted USPIO for the localization and imaging by MRI of tumor or angiogenic vasculature are of great interest,[30] but their production is still an ongoing challenge.[4,25] In this context we wanted to propose the clip photochemistry strategy in the aqueous media as a safe and controllable process.

In this paper we first present the development of the clip photochemistry in water on PEG and we explore several factors. The NHS functionality on PEG is assayed with molecular probes counted by quantitative ^{19}F NMR spectroscopy (^{19}F qNMR), liquid scintillation counting (LSC), and elementary analysis (EA). Then, we apply it to graft RGD and RGDp on PEGylated USPIO (USPIO-PEG)[31] in water environment. The RGD and RGDp conjugated USPIO-PEG are thoroughly characterized by LSC, EA, photo correlation

DOI: 10.1021/acs.bioconjchem.5b00041
Bioconjugate Chem. 2015, 26, 822−829

spectroscopy (PCS), transmission electron microscopy (TEM), magnetometric and relaxometric profiles, and their magnetic labeling abilities are assessed in vitro toward Jurkat cells, a model of leukemia expressing integrin $\alpha_v\beta_3$.

RESULTS AND DISCUSSION

1. Clip Photochemistry in Aqueous Media. *1.1. PEG Functionalization.* The principle of the photografting process is depicted in Scheme 1. An aqueous solution containing MePEG and *O*-succinimidyl-4-(1-azi-2,2,2-trifluoroethyl)-benzoate (NHS-TPD clip) is submitted to black light (350 nm). Then, the activated diazirine function, by loss of dinitrogen, gives a stabilized trifluoromethylphenylcarbene which inserts into any C−H bond situated in its close vicinity, leading to a PEG with pendent NHS ester (Me-PEG-*g*-NHS). This desired singlet carbene pathway can be disturbed by several side reactions particularly in water.[32−36] A detailed review of the possible parasitic reactions and the experimental choices made to avoid them is given in the Supporting Information. Most notably, (i) acetonitrile was added for the TPD clip solubility and for the stabilization of the singlet carbene;[37] (ii) the formation of a stable diazo compound was avoided with a diazirine concentration under 10 mM;[35,36] and (iii) the insertion in the C−H bond was favored by increasing PEG concentration in the presence of an excess of TPD clip, but (iv) with a constant PEG:TPD clip molar ratio of 0.5.

As seen in Figure 1 the whole process is followed by ^{19}F NMR. We observe the disappearance of the diazirine peak at −65 ppm after 15 min of irradiation and consequently choose an irradiation time of 30 min. Contrary to the complex ^{19}F NMR profiles obtained in the solid phase, here we observe three main peaks (Figure 1B) at −73.2, −77.6, and −83.8 ppm in the proportion 40%, 35%, and 25%, respectively. From the literature[33,38] we can guess that the peak at −77.6 ppm belongs to the carbene adduct with water and the peak at −73.2 ppm corresponds to the desired product of carbene insertion on PEG. This is confirmed by the fact that it is the only one to be kept after all the treatments (Figure 1C). We employed 3,5-bis-trifluoromethyl-benzylamine (Tag F_6, Scheme 1) as a molecular probe to assay the NHS reactivity after grafting. It is a good mimic of our RGD peptidomimetics leading to identical functionalization rates that are determined with a well-defined ^{19}F quantitative NMR (^{19}F qNMR) protocol using trifluoroethanol as internal standard[6] (Figure 1C). To eliminate the contribution of unbound Tag F_6 we subtract the value obtained on a "non-irradiated" control sample treated in parallel to the main "irradiated sample" (see Experimental Section). Hence, we achieve a real amount of covalently bound TagF_6 that indicates whether the grafting is efficient or not.

Figure 2 shows the results recorded under two experimental conditions. Under condition A we used the concentration upper limit for the diazirine clip mentioned before (i.e., 10 mM) and, to keep a 0.5 molar ratio, a PEG concentration of 20 mM. We obtained a rate of 117 μmol of Tag F_6 per gram of PEG on the irradiated sample and of 61 μmol/g on the nonirradiated one. This means a real amount of 56 μmol/g, corresponding to the functionalization of 22% of the initial quantity of NHS-TPD clip. It also signifies one grafted PEG chain over ten. Under experimental condition B, we performed the photografting in less concentrated solution, and as seen in Figure 2, we obtained a grafting rate of 27 μmol/g on the irradiated sample and of 5 μmol/g on the nonirradiated one. This corresponds to 22 μmol/g of covalently grafted Tag F_6

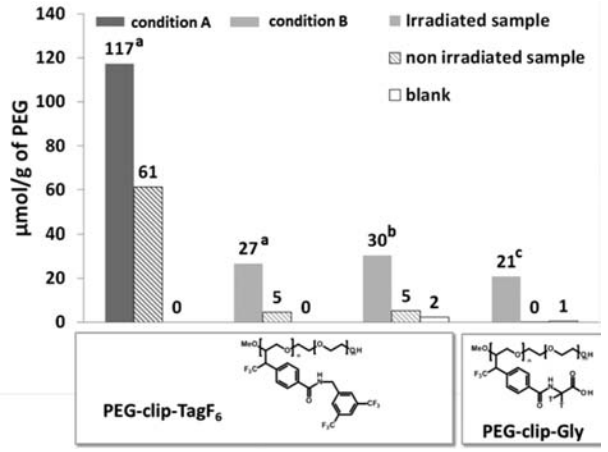

Figure 2. Grafting rates obtained on PEG_{2k} with different initial conditions (condition A: [PEG_{2k}] = 20 mM, [TDP clip] = 10 mM; condition B: [PEG_{2k}] = 8 mM, [TDP clip] = 4 mM), different molecular probes (Tag F_6 and ^{3}H-Glycine) and different quantification techniques ([a]Fluorine qNMR, [b]Elementary Analysis, [c]Liquid scintillation counting).

and a yield of 9% regarding the initial quantity of NHS-TPD clip, meaning that we have functionalized 1 chain over 20. Due to the presence of fluorine those results were easily checked by elementary analysis (EA) (Figure 2) and we found almost the same grafting rates and yields (i.e., real amount of 25 μmol/g and yield of 10%). We also assayed the reactivity of Me-PEG-*g*-NHS with tritiated glycine (^{3}H-Gly, Scheme 1) to mimic the grafting of the pentapeptide NH_2-Gly-Arg-Gly-Asp-Ser-OH (GRGDS). We found by liquid scintillation counting (LSC) a glycine rate of 21 μmol/g on the irradiated sample and nothing on the controls (Figure 2) which means a yield of 9% identical to the one obtained with Tag F_6. By comparison of conditions A and B, better results in terms of yield were obtained with the more concentrated solution, but also higher level of physisorption of molecular probe, as seen on the control sample (Figure 2). Anyway, all of these results evidence an efficient and reproducible photografting of NHS-TPD clip on PEG in aqueous solution, but with low yield in comparison to the one obtained in solid phase, which is usually around 90%.[6] As we have checked by ^{1}H NMR that the reactivity of NHS ester was not attained by the irradiation in water (see Supporting Information), we can attribute this drop of yield to the side reactions of carbene. These results of photografting on PEG in aqueous solution pave the way for the grafting of biomolecules to PEG corona of nanoparticles and to the analytical tools that can be used for their quantification.

1.2. Synthesis of Bioconjugated USPIO-PEG. 1.2.1. Grafting of ^{3}H-Glycine. Clip photochemistry on PEGylated ultrasmall iron oxide particles (USPIO-PEG)[31] required slight modifications mostly due to the dark red solution that limits the transmission of light. We overcame this problem by (i) the dilution with acetonitrile, (ii) a vigorous stirring that disperses the solution as a thin layer on the surface of the flask, and (iii) a prolonged irradiation time (2 h). Superparamagnetic particles cannot be used in NMR, so we assayed the NHS functionalization rates with ^{3}H-Gly. By LSC we recorded a grafting rate of 21 μmol of ^{3}H-Gly per gram of USPIO-PEG and only 2 μmol/g on the non-irradiated sample (Figure 3). This applies for a covalent grafting rate of 19 μmol/g and an estimated yield of 15%. For comparison purposes, the same

DOI: 10.1021/acs.bioconjchem.5b00041
Bioconjugate Chem. 2015, 26, 822−829

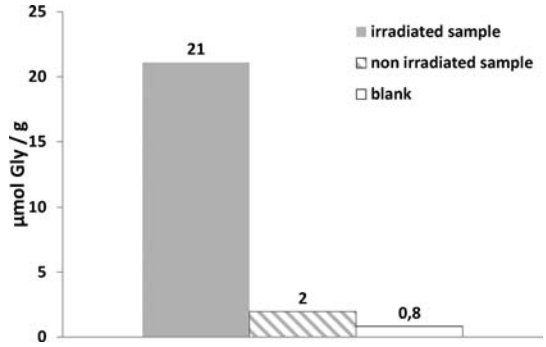

Figure 3. Grafting rates of ^{3}H-Glycine on USPIO-PEG determined by LSC ([USPIO-PEG] = 92 mM, [PEG] = 0.7 mM).

photografting procedure was also attempted twice on freeze-dried samples of USPIO-PEG, and in both cases, very small amounts ($\leq$1 μmol/g) of molecular probe were measured with nonsignificant differences between the main sample and the controls (see Figure S4 in Supporting Information). Moreover, the redispersion of the functionalized nanoparticles in solution led to a lot of aggregates that needed to be filtered off. It thus seems obvious that for this kind of stealth nanoparticles which cannot suffer to be dried, the direct photografting in aqueous solution is a method of choice.

1.2.2. Grafting of RGD and RGDp. The final aim of the study was to develop a convenient way to produce USPIO-PEG particles conjugated with the biomolecules GRGDS pentapeptide (RGD) and peptidomimetics of the RGD sequence (RGDp). We synthesized two RGDp based on the same tyrosine scaffold equipped with a caproyl spacer but differing only by their basic moieties (compound 7 in Scheme S1 and compound **12** in Scheme S2 in Supporting Information). The caproyl spacer made them easier to synthesize and to handle in comparison with the oligoethylene glycol (OEG) spacer used in previous study.[27] For the purpose of the study, we choose RGDp with the naphthyridine function (compound **12**), since it is known to give the highest affinity for $\alpha_v\beta_3$ integrin (see Table S1 in Supporting Information).

RGD and RGDp were grafted on USPIO-PEG as depicted in Scheme 2, giving USPIO-PEG-RGD and USPIO-PEG-RGDp, respectively. Thanks to the presence of a CF_3 tag on the RGDp molecule, a final grafting rate of 41 μmol per gram of USPIO-PEG-RGDp and a grafting yield of 30% was obtained by EA.

Scheme 2. Clip Photochemistry Grafting of RGD and RGDp on USPIO-PEG Nanoparticles

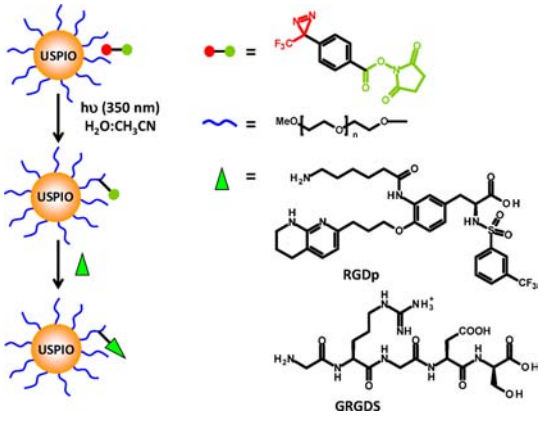

The mean core diameter of the particles, determined by TEM, was evaluated to be 7.7−7.9 nm. In each case, the presence of a single population characterized by a quite narrow size distribution was identified (Figure 4). It can be noted that the photochemical treatment does not affect the size of the magnetic iron oxide core.

2. Magnetic Properties of the Bioconjugated NPs. Next we had to control whether the grafting methodology impairs the magnetic properties of the USPIO-PEG nanoparticles. We determined their hydrodynamic size, longitudinal relaxivity (r_1), and transverse relaxivity (r_2) (Table 1). A slight increase in size is observed for USPIO-PEG-RGDp, whereas USPIO-PEG-RGD seems to suffer a decrease. This might be explained by the difference in size and in hydrophilicity of the ligands. On one hand, we have a bulky (920 g·mol^{-1}) and lipophilic RGDp, and on the other hand a smaller (450 g·mol^{-1}) and more hydrophilic peptide (GRGDS). Consequently, the former might be repelled far from the charged surface of the nanoparticles and so provokes an increase of the hydrodynamic radius, whereas the latter might be attracted by these charges leading to a decrease of the hydrodynamic size. The higher transverse relaxivities observed for USPIO-PEG-RGDp are probably due to the slight tendency of these nanoparticles to aggregate.

The nuclear magnetic resonance dispersion (NMRD) profiles, shown in Figure 5, confirm that the magnetic properties are maintained after the clip photochemistry process and that no significative change is observed. Table 2 gives the magnetization and the radius obtained by fitting of the NMRD curves. With all these observations it seems clear that the targeted USPIO are suitable for biomedical applications.

3. Targeting Properties of the Bioconjugated NPs. In our previous study[27] we tested the magnetic labeling of cells with Jurkat T lymphocyte cells which are considered a good model for the study of $\alpha_v\beta_3$ integrin expression.[39−41] When stimulated with phorbol 12-myristate 13-acetate (PMA) they overexpress $\alpha_v\beta_3$ integrin. We incubated stimulated and non-stimulated Jurkat cells with the USPIO nanoparticles for 2 h, then washed out the excess and measured the transverse relaxation rate R_2 at 60 MHz. We evidenced a good cell labeling with the two bioconjugated nanoparticles which are more efficiently trapped by the activated cells. Indeed, as seen in Figure 6, the relaxation rate measured is more than twice as great when the cells are stimulated and overexpress integrin receptors. In comparison with the results previously obtained in the same in vitro experiment, with non-PEGylated USPIO,[27] here the native USPIO-PEG were not captured by stimulated nor by unstimulated cells and so reveal a real stealthiness. Therefore, with the conjugated particles we observed an enhanced cellular uptake characterized by a pronounced effect on R_2 which is increased more than 10 times (i.e., 10 times with USPIO-PEG-RGD and 14 times with USPIO-PEG-RGDp). Moreover, as this effect is amplified by the augmentation of $\alpha_v\beta_3$ integrin it could be attributed to a receptor dependent endocytosis. As these USPIO-PEGs have already shown a long circulating behavior in vivo,[31] this added targeting ability makes them good candidates for sensitive MRI applications.

CONCLUSIONS

In this study we have expanded the scope of a post-functionalization methodology, the so-called "clip photochemistry", usually dedicated to dry materials and clean surfaces, to aqueous solutions. It allowed us to transform a

DOI: 10.1021/acs.bioconjchem.5b00041
Bioconjugate Chem. 2015, 26, 822−829

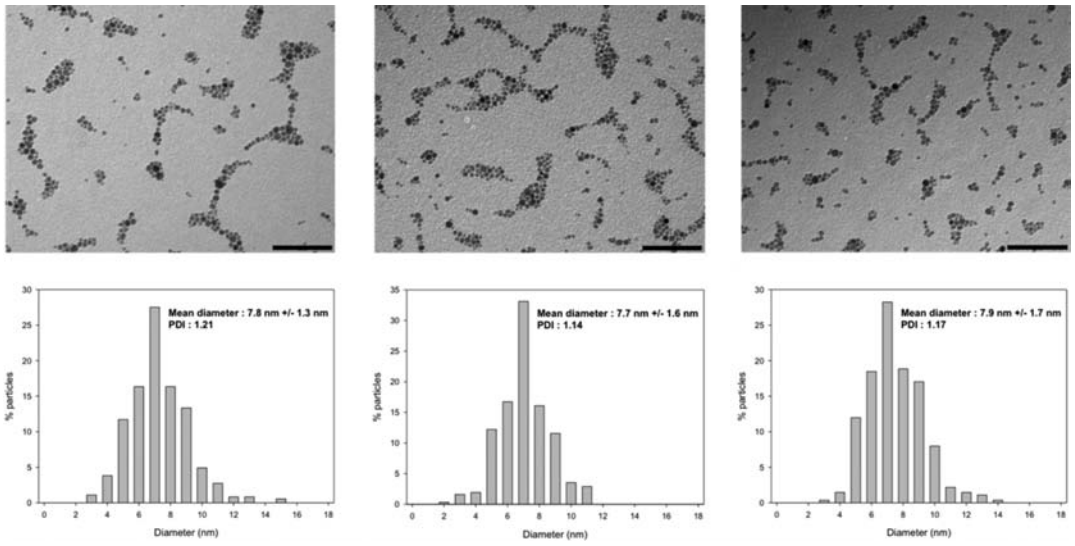

Figure 4. TEM pictures of the USPIO-PEG (left), USPIO-PEG-RGD (middle), and USPIO-PEG-RGDp NPs (right). The size distribution was obtained after a count of more than 300 particles. PDI: polydispersity index. Scale bar = 100 nm.

Table 1. Comparison of USPIO-PEG Physicochemical Parameters

		r_1[a] (nM^{-1} s^{-1})	r_2[b] (nM^{-1} s^{-1})	r_h[c] (nm)
USPIO-PEG	20 MHz	30.4	62.2	24
	60 MHz	11.2	59.7	
USPIO-PEG-RGD	20 MHz	31.9	73.9	17
	60 MHz	14.8	68.9	
USPIO-PEG-RGDp	20 MHz	30.1	106.5	34
	60 MHz	12.2	103.3	

[a]Longitudinal relaxivity determined at 37 °C. [b]Transverse relaxivity determined at 37 °C. [c]Hydrodynamic size determined by photon correlation spectroscopy (PCS).

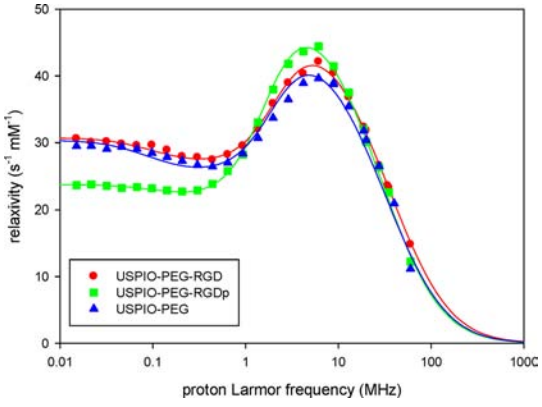

Figure 5. NMRD profiles of USPIO-PEG-RGDp, USPIO-PEG-RGD, and USPIO-PEG (without vector).

Table 2. Parameters (Magnetization and Radius) Obtained from the Theoretical Fitting of the NMRD Profiles

	M_{sat} (Am^2/kg)	r (nm)
USPIO-PEG-RGD	50.2 ± 0.3	5.6 ± 0.1
USPIO-PEG-RGDp	46.6 ± 0.3	6.4 ± 0.1
USPIO-PEG	46.9 ± 0.3	5.9 ± 0.1

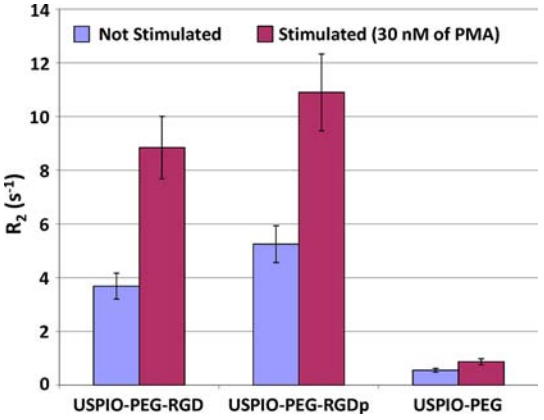

Figure 6. Relaxation time (R_2) measured on Jurkat cells treated with the different USPIO-PEG.

commercial unreactive polymer, presently a 2 kDa PEG, into a material bearing reactive functions along its backbone following a simple protocol. We have exemplified the technique by grafting in water environment several molecular probes onto the polymer and we evidenced the main parameters and limitations of the photografting in this media. As a very smooth and clean chemical process, it also opens the door to a great versatility; for instance, we can imagine introducing several other functions such as maleimide, clickable functions or leaving groups simply by using photoactivable clips bearing these groups.

However, from our point of view, the most interesting application of this photografting in water would be for the derivatization of nanosystems and more specifically "stealth" nanoparticles. The development of a clean chemistry for the introduction of targeting ligands on external coronas of nanoparticles is a great challenge in itself. For instance, this is a long-term research challenge of our groups to produce stealth USPIO nanoparticles that could specifically map tumor tissues.[27,31] In the present work, with the clip photochemistry in water, we were able to introduce highly specific ligands of $\alpha_v\beta_3$ integrins (a marker of certain cancer cells and endothelial tissues) on PEGylated USPIO nanoparticles without interfering

DOI: 10.1021/acs.bioconjchem.5b00041
Bioconjugate Chem. 2015, 26, 822−829

on their magnetic abilities. Moreover, with the in vitro model of Jurkat cells, we evidenced a good stealthiness of native PEGylated particles and we showed that the conjugated ones are able to label cells expressing the targeted integrins ten times more than nonconjugated ones. These furtive targeted USPIO would be of great interest for sensitive MRI applications in cancer treatment and detection.

EXPERIMENTAL SECTION

All solvents used were of analytical grade. All chemicals (unless stated) were purchased from Sigma-Aldrich and Acros. α-Methoxy-ω-hydroxyl-poly(ethylene glycol) 2000 kDa (PEG 2k) was purchased from Fluka. Dialysis membranes RC, MWCO 2000 Da and CE 7, MWCO 500 and 10000 were obtained from Spectra/Por. The RGD peptidomimetics were synthesized in our laboratory following procedures described in the Supporting Information. *O*-Succinimidyl-4-(1-azi-2,2,2-trifluoroethyl)benzoate (NHS-TPDclip) was prepared as previously published.[6] PEGylated ultrasmall iron oxide particles were prepared as described elsewhere[31] and are presented in an aqueous suspension with a [Fe] of 185 mM. Glycine [2-^{3}H] pack size 1 mCi was purchased from American Radiolabeled Chemicals. ^{1}H (500 MHz) and ^{13}C (125 MHz) NMR spectra were recorded on a Bruker Avance 500 spectrometer.^{19}F (282.09 MHz) NMR spectra were recorded on a Bruker Avance II spectrometer. Spectra were obtained in D_2O or CD_3CN at room temperature. Chemical shifts are reported in ppm and are calibrated at 0 ppm on the TMSP and $CFCl_3$ signals for ^{1}H NMR and ^{19}F NMR, respectively. Irradiations were performed in a homemade reactor (rotating quartz flask of 15 mL) with 3 × 8 W BLB lamps (360 nm) placed at a distance of 4.5 cm. Liquid Scintillation Counting (LSC) was performed on a TriCarb 1600 TR liquid scintillation analyzer (PerkinElmer instrument, San Diego, CA).

Photografting of PEG in Aqueous Conditions (PEG-*g*-NHS). Samples were prepared by adding the required volume of a 20 mM NHS-TPD clip solution (prepared by dissolving 13 mg NHS-TPD clip in 2 mL of CH_3CN) in 2 mL of a PEG 2000 kDa solution in H_2O/CH_3CN in order to have a PEG:NHS-TPD clip ratio of 0.5. Then, the mixed solution was irradiated for 30 min. The completion of the irradiation was followed by ^{19}F NMR after addition of few drops of D_2O.

Photografting on PEGylated USPIO (USPIO-PEG-NHS). A sample was prepared by adding 1 mL of CH_3CN and 300 μL of a 5.5 mM NHS-TPD clip solution (prepared by dissolving 9 mg NHS-TPD clip in 5 mL of CH_3CN) to 1 mL of USPIO-PEG (185 mM, Rh = 24 nm, PEG 2.5 w%). Then the mixed solution was irradiated for 2 h.

Preparation of PEG-clip-TagF_6 and PEG-clip-Gly. To the solution of PEG-clip-NHS prepared above, 2 mL of a solution of the desired compound (3,5-bis-trifluoromethyl-benzylamine (TagF_6) 10 mM or Glycine:^{3}H-Glycine 10:5.10^{-5} mM) in 0.1 M phosphate buffer (PB):CH_3CN (1:1, v/v) at pH 8.0, is added and the mixture is shaken for 24 h at 20 °C.

The samples treated with TagF_6 were dialyzed (MWCO 500) for 100−130 h against water with replacement of the water every 8−12 h. Then, they were lyophilized, solubilized in CH_2Cl_2, and filtered on PTFE Acrodisc filters (0.2 mm) and dried under vacuum. The solid residue was solubilized in 0.1 mL of MeOH and precipitated twice in 2 mL of isopropyl ether before being dried by azeotropic distillation with CH_3CN. The samples treated with ^{3}H-glycine were dialyzed (MWCO 500, for 100−130 h) against water.

The same protocol was applied with unlabeled Gly (^{1}H-Gly) for the preparation of samples analyzed by ^{1}H NMR.

Preparation of USPIO-PEG-^{3}H-Gly, USPIO-PEG-RGD, and USPIO-PEG-RGDp. To the solution of USPIO-PEG-NHS prepared above, 1 mL of a solution of the desired compound (Glycine:^{3}H-Glycine 10:5.10^{-5} mM, RGDp 30 mM and GRGDS 50 mM) in PB:CH_3CN (1:1, v/v) at pH 8.0, is added, and the mixture is shaken for 3 days at 20 °C.

The samples were dialyzed (SpectraPor CE, MWCO 2000) for 160 h against water with replacement of the water every 8−12 h. The solution obtained was then concentrated to 1−2 mL by ultracentrifugation (Amicon Ultra 3000).

Determination of the Grafting Rates and Yields. In parallel to the main sample, irradiated in the presence of the NHS-TPD-Clip, several reference samples were prepared to control the nonspecific adsorption versus covalent grafting. They are designed as non-irradiated (standard protocol omitting the UV irradiation) and blank (standard photografting protocol omitting the NHS-TPD clip). The final grafting rate, defined as the real amount of covalently bound molecular probe, was deduced from the subtraction of the grafting rate on the nonirradiated sample to the one on the irradiated sample. Grafting yield is defined as the ratio between the final grafting rate to the initial amount of NHS TPD Clip.

Tag F_6 rates on PEG-clip-Tag F_6 samples were determined by quantitative ^{19}F NMR as described in ref 6 or by elementary analysis (EA) with eq1

$$n_{\mathrm{TagF_6}} = \left(\frac{\%\mathrm{F}}{\mathrm{MW_F} \times n_\mathrm{F} \times 100} \times 10^6 \right) \quad (1)$$

where $n_{\mathrm{TagF_6}}$ is the grafting rates of Tag F_6 in μmol/g, %F the percentage of fluorine determined by EA, $\mathrm{MW_F}$ is the molecular weight of fluorine, and n_F is the number of fluorine in Tag F_6.

RGDp rates on USPIO-PEG-RGDp samples were determined by EA with eq 1.

^{3}H-Gly rates on PEG-clip-^{3}H-Gly and USPIO-PEG-^{3}H-Gly were determined by liquid scintillation counting (LSC). 1 mL of the final sample solution was poured in 5 mL of AQUALUMA in an individual PE vials and counted by LSC to obtain the DPM value of the sample. The amount of ^{3}H-Gly in the sample was calculated from the DPM value by using a calibration curve. The quantity of solid contained in 1 mL of the final sample solution was determined by weighting the dry residue obtained after evaporation under vacuum. Consequently ^{3}H-Gly rates given in μmol/g were calculated by dividing the LSC quantity of ^{3}H-Gly by the solid residue mass.

Physicochemical Characterization. Hydrodynamic size measurement was carried out by photon correlation spectroscopy (PCS) on a Malvern system (Zêtasizer Nanoseries ZEN 3600, United Kingdom) using laser He−Ne (633 nm).

Nuclear magnetic relaxation dispersion (NMRD) profiles were recorded with a field cycling relaxometer (STELAR, Mede, Italy) measuring the longitudinal relaxivity (r_1) in a magnetic field range extending from 0.24 mT to 1 T at 37 °C. Longitudinal (r_1) and transverse (r_2) relaxivity measurements at 0.47 and 1.41 T were performed on Minispec Mq 20 and Mq 60 spin analyzers (Bruker, Germany), respectively. The fitting of the NMRD profiles by a theoretical relaxation model allows the determination of the crystal radius (r) and the specific magnetization (M_S) as described elsewhere.[42,43]

The total iron concentration was determined by the measurement of the longitudinal relaxation rate R_1 according

DOI: 10.1021/acs.bioconjchem.5b00041
Bioconjugate Chem. 2015, 26, 822−829

to the method previously described[44] after microwave digestion (MLS-1200 Mega, Milestone, Analis, Namur, Belgium). Briefly, the samples were mineralized and the R_1 values of the resulting solutions were recorded at 0.47 T and 37 °C, which allowed the determination of iron concentration using eq 2:

$$[\mathrm{Fe}] = (R_1^{\mathrm{sample}} - R_1^{\mathrm{diam}}) \times 0.0915 \quad (2)$$

where R_1^{diam} in s^{-1} is the diamagnetic relaxation rate of water at acidic pH (0.36 s^{-1}) and 0.0915 in s.mM is the slope of the calibration curve.

Transmission electron microscopy (TEM) was used to obtain detailed morphological information on the samples and was carried out using a Fei Tecnai 10 microscope (Oregon, USA) operating at an accelerating voltage of 80 kV. The samples were prepared by placing a drop of diluted suspension of iron oxide nanoparticles on a copper grid (300 mesh), allowing the liquid to dry in air at room temperature. The statistical analysis of the TEM images was performed by iTEM (Germany) on multiple images for each sample. The mean diameter, the standard deviation, and the polydispersity index (PDI) were calculated by measuring the particle diameter. The number of nanoparticles counted ranged from 300 to 400.

Cell Cultures. The magnetic labeling of cells expressing $\alpha_v\beta_3$ integrin was performed with Jurkat T lymphocytes. These leukemic cells are known to express the $\alpha_v\beta_3$ receptor under stimulation with phorbol 12-myristate 13-acetate (PMA, 30 nM, 48h, 37 °C, 5% CO_2). Cells (10^6 cells/mL), stimulated or not (negative control), were incubated in USPIO-peptide suspensions (0.5 mM) during 2 h at 25 °C. After washing out the excess particles, cells were seeded in a gelatin matrix for measuring T_2 (CPMG pulse sequence, Bruker Minispec Mq-60, 60 MHz, 15 °C). The efficiency of USPIO capture by cells is determined by the R_2^{norm} values (where $R_2 = 1/T_2$, while R_2^{norm} is the normalized R_2 which is calculated by subtracting the R_2 of cells free of USPIO from the cells incubated with iron oxide nanoparticles), the highest values corresponding to the best cell targeting.[40,41] These experiments have been done in triplicate.

■ ASSOCIATED CONTENT

Supporting Information

Process elaboration to favor the C−H insertion of carbene, ^{1}H NMR study of the NHS-reactivity, Photografting in the solid phase on dried USPIO-PEG, RGD peptidomimetics biological testings, RGD peptidomimetics synthesis and full characterizations. This material is available free of charge via the Internet at http://pubs.acs.org.

■ AUTHOR INFORMATION

Corresponding Author

*E-mail: jacqueline.marchand@uclouvain.be. Tel:+32-10-472740. Fax:+32-10-474168.

Notes

The authors declare no competing financial interest.

■ ACKNOWLEDGMENTS

Benedicte Valet and Camille Bouillon are acknowledged for their contribution to the RGDp synthesis and protocol description (in Supporting Information). Coralie Thirifays is acknowledged for her help in cell cultures. The ARC (research contract AUWB-2010—10/15-UMONS-5), the FNRS, the Region Wallone, ENCITE program, the COST TD1004 (Theranostics imaging and therapy: an action to develop novel nanosized systems for imaging-guided drug delivery), the UIAP VII program, the European Network of Excellence EMIL (European Molecular Imaging Laboratories) program LSCH-2004-503569 and the Center for Microscopy and Molecular Imaging (CMMI, supported by the European Regional Development Fund and the Walloon Region) are thanked for their support.

■ REFERENCES

(1) Cheng, Z., Al Zaki, A., Hui, J. Z., Muzykantov, V. R., and Tsourkas, A. (2012) Multifunctional nanoparticles: cost versus benefit of adding targeting and imaging capabilities. *Science 338*, 903−910.

(2) Crommelin, D. J. A., and Florence, A. T. (2013) Towards more effective advanced drug delivery systems. *Int. J. Pharm. 454*, 496−511.

(3) Muro, S. (2012) Challenges in design and characterization of ligand-targeted drug delivery systems. *J. Controlled Release 164*, 125−137.

(4) Turcheniuk, K., Tarasevych, A. V., Kukhar, V. P., Boukherroub, R., and Szunerits, S. (2013) Recent advances in surface chemistry strategies for the fabrication of functional iron oxide based magnetic nanoparticles. *Nanoscale 5*, 10729−10752.

(5) Venditto, V. J., and Szoka, F. C., Jr. (2013) Cancer nanomedicines: So many papers and so few drugs! *Adv. Drug Delivery Rev. 65*, 80−88.

(6) Pourcelle, V., Le Duff, C. S., Freichels, H., Jérôme, C., and Marchand-Brynaert, J. (2012) Clickable PEG conjugate obtained by "clip" photochemistry: Synthesis and characterization by quantitative ^{19}F NMR. *J. Fluorine Chem. 140*, 62−69.

(7) Freichels, H., Pourcelle, V., Le Duff, C. S., Marchand-Brynaert, J., and Jérôme, C. (2011) "Clip" and "Click" chemistries combination: toward easy PEGylation of degradable aliphatic polyesters. *Macromol. Rapid Commun. 32*, 616−621.

(8) Brunner, J., Senn, H., and Richards, F. M. (1980) 3-Trifluoromethyl-3-phenyldiazirine. A new carbene generating group for photolabeling reagents. *J. Biol. Chem. 255*, 3313−18.

(9) Keana, J. F. W., and Cai, S. X. (1990) New reagents for photoaffinity labeling: synthesis and photolysis of functionalized perfluorophenyl azides. *J. Org. Chem. 55*, 3640−3647.

(10) Blencowe, A., and Hayes, W. (2005) Development and application of diazirines in biological and synthetic macromolecular systems. *Soft Matter 1*, 178−205.

(11) Coco, R., Plapied, L., Pourcelle, V., Jérôme, C., Brayden, D. J., Schneider, Y.-J., and Préat, V. (2013) Drug delivery to inflamed colon by nanoparticles: Comparison of different strategies. *Int. J. Pharm. 440*, 3−12.

(12) Danhier, F., Pourcelle, V., Marchand-Brynaert, J., Jérôme, C., Feron, O., and Préat, V. (2012) Chapter eight - targeting of tumor endothelium by RGD-grafted PLGA-nanoparticles. *Methods Enzymol. 508*, 157−175.

(13) Freichels, H., Pourcelle, V., Auzély-Velty, R., Marchand-Brynaert, J., and Jérôme, C. (2012) Synthesis of poly(lactide-co-glycolide-co-ε-caprolactone)-graft-mannosylated poly(ethylene oxide) copolymers by combination of "clip" and "click" chemistries. *Biomacromolecules 13*, 760−768.

(14) Zhang, Z., Lai, Y., Yu, L., and Ding, J. (2010) Effects of immobilizing sites of RGD peptides in amphiphilic block copolymers on efficacy of cell adhesion. *Biomaterials 31*, 7873−7882.

(15) Hashimoto, M., and Hatanaka, Y. (2008) Recent progress in diazirine-based photoaffinity labeling. *Eur. J. Org. Chem. 2008*, 2513−2523.

(16) Platz, M., Admasu, A. S., Kwiatkowski, S., Crocker, P. J., Imai, N., and Watt, D. S. (1991) Photolysis of 3-aryl-3-(trifluoromethyl)-diazirines: a caveat regarding their use in photoaffinity probes. *Bioconjugate Chem. 2*, 337−341.

(17) Blencowe, A., Blencowe, C., Cosstick, K., and Hayes, W. (2008) A carbene insertion approach to functionalised poly(ethylene oxide)-based gels. *React. Funct. Polym. 68*, 868−875.

DOI: 10.1021/acs.bioconjchem.5b00041
Bioconjugate Chem. 2015, 26, 822−829

(18) Mehenni, H., Pourcelle, V., Gohy, J.-F., and Marchand-Brynaert, J. (2012) Synthesis and application of new photocrosslinkers for poly(ethylene glycol). *Aust. J. Chem. 65*, 193−201.
(19) Pauloehrl, T., Delaittre, G., Winkler, V., Welle, A., Bruns, M., Börner, H. G., Greiner, A. M., Bastmeyer, M., and Barner-Kowollik, C. (2012) Adding spatial control to click chemistry: phototriggered Diels−Alder surface (bio)functionalization at ambient temperature. *Angew. Chem., Int. Ed. 51*, 1071−1074.
(20) Tischer, T., Rodriguez-Emmenegger, C., Trouillet, V., Welle, A., Schueler, V., Mueller, J. O., Goldmann, A. S., Brynda, E., and Barner-Kowollik, C. (2014) Photo-patterning of non-fouling polymers and biomolecules on paper. *Adv. Mater. 26*, 4087−4092.
(21) Arumugam, S., Orski Sara, V., Mbua Ngalle, E., McNitt, C., Boons, G.-J., Locklin, J., and Popik Vladimir, V. (2013) *Pure Appl. Chem.*, 1499.
(22) Arumugam, S., and Popik, V. V. (2014) Sequential "Click" − "Photo-Click" cross-linker for catalyst-free ligation of azide-tagged substrates. *J. Org. Chem. 79*, 2702−2708.
(23) Danhier, F., Vroman, B., Lecouturier, N., Crokart, N., Pourcelle, V., Freichels, H., Jérôme, C., Marchand-Brynaert, J., Feron, O., and Préat, V. (2009) Targeting of tumor endothelium by RGD-grafted PLGA-nanoparticles loaded with Paclitaxel. *J. Controlled Release 140*, 166−173.
(24) Fievez, V., Plapied, L., des Rieux, A., Pourcelle, V., Freichels, H., Wascotte, V., Vanderhaeghen, M.-L., Jerôme, C., Vanderplasschen, A., Marchand-Brynaert, J., et al. (2009) Targeting nanoparticles to M cells with non-peptidic ligands for oral vaccination. *Eur. J. Pharm. Biopharm. 73*, 16−24.
(25) Elias, D. R., Poloukhtine, A., Popik, V., and Tsourkas, A. (2013) Effect of ligand density, receptor density, and nanoparticle size on cell targeting. *Nanomedicine 9*, 194−201.
(26) Valencia, P. M., Hanewich-Hollatz, M. H., Gao, W., Karim, F., Langer, R., Karnik, R., and Farokhzad, O. C. (2010) Effects of ligands with different water solubilities on self-assembly and properties of targeted nanoparticles. *Biomaterials 32*, 6226−6233.
(27) Rerat, V., Laurent, S., Burtéa, C., Driesschaert, B., Pourcelle, V., Vander Elst, L., Muller, R. N., and Marchand-Brynaert, J. (2010) Ultrasmall particle of iron oxide - RGD peptidomimetic conjugate: synthesis and characterisation. *Bioorg. Med. Chem. Lett. 20*, 1861−1865.
(28) Bridot, J.-L., Stanicki, D., Laurent, S., Boutry, S., Gossuin, Y., Leclère, P., Lazzaroni, R., Vander Elst, L., and Muller, R. N. (2013) New carboxysilane-coated iron oxide nanoparticles for nonspecific cell labelling. *Contrast Media Mol. Imaging 8*, 466−474.
(29) Danhier, F., Le Breton, A., and Préat, V. (2012) RGD-based strategies to target alpha(v) beta(3) integrin in cancer therapy and diagnosis. *Mol. Pharmaceutics 9*, 2961−2973.
(30) Tsourkas, A., Shinde-Patil, V. R., Kelly, K. A., Patel, P., Wolley, A., Allport, J. R., and Weissleder, R. (2005) In vivo imaging of activated endothelium using an anti-VCAM-1 magnetooptical probe. *Bioconjugate Chem. 16*, 576−581.
(31) Stanicki, D., Boutry, S., Laurent, S., Wacheul, L., Nicolas, E., Crombez, D., Vander Elst, L., Lafontaine, D. L. J., and Muller, R. N. (2014) Carboxy-silane coated iron oxide nanoparticles: a convenient platform for cellular and small animal imaging. *J. Mater. Chem. B 2*, 387−397.
(32) McAllister, G. D., Perry, A., and Taylor, R. J. K. (2008) Diaziridines and Diazirines, in *Comprehensive Heterocyclic Chemistry III* (Alan, R. K., Christopher, A. R., Eric, F. V. S., and Richard, J. K. T., Eds.) pp 539−557, Elsevier, Oxford.
(33) Raimer, B., and Lindel, T. (2013) Photoactivation of (p-methoxyphenyl)(trifluoromethyl)diazirine in the presence of phenolic reaction partners. *Chem.—Eur. J. 19*, 6551−6555.
(34) Song, M.-G., and Sheridan, R. S. (2011) Effects of CF3 groups and charged substituents on singlet carbene stabilities−a density functional theory study. *J. Phys. Org. Chem. 24*, 889−893.
(35) Hashimoto, M., and Hatanaka, Y. (2006) Practical conditions for photoaffinity labeling with 3-trifluoromethyl-3-phenyldiazirine photophore. *Anal. Biochem. 348*, 154−156.
(36) Mayer, T., and Maier, M. E. (2007) Design and synthesis of a tag-free chemical probe for photoaffinity labeling. *Eur. J. Org. Chem. 2007*, 4711−4720.
(37) Wang, J., Kubicki, J., Gustafson, T. L., and Platz, M. S. (2008) The dynamics of carbene solvation: an ultrafast study of p-biphenylyltrifluoromethylcarbene. *J. Am. Chem. Soc. 130*, 2304−2313.
(38) Hosoya, T., Hiramatsu, T., Ikemoto, T., Nakanishi, M., Aoyama, H., Hosoya, A., Iwata, T., Maruyama, K., Endo, M., and Suzuki, M. (2004) Novel bifunctional probe for radioisotope-free photoaffinity labeling: compact structure comprised of photospecific ligand ligation and detectable tag anchoring units. *Org. Biomol. Chem. 2*, 637−641.
(39) Burtea, C., Laurent, S., Port, M., Lancelot, E., Ballet, S., Rousseaux, O., Toubeau, G., Vander Elst, L., Corot, C., and Muller, R. N. (2009) Magnetic resonance molecular imaging of vascular cell adhesion molecule-1 expression in inflammatory lesions using a peptide-vectorized paramagnetic imaging probe. *J. Med. Chem. 52*, 4725−4742.
(40) Chen, Z., Ahonen, M., Hämäläinen, H., Bergelson, J. M., Kähäri, V.-M., and Lahesmaa, R. (2002) High-efficiency gene transfer to primary T lymphocytes by recombinant adenovirus vectors. *J. Immunol. Methods 260*, 79−89.
(41) Huang, S., Endo, R. I., and Nemerow, G. R. (1995) Upregulation of integrins alpha v beta 3 and alpha v beta 5 on human monocytes and T lymphocytes facilitates adenovirus-mediated gene delivery. *J. Virol. 69*, 2257−63.
(42) Laurent, S., Forge, D., Port, M., Roch, A., Robic, C., Vander Elst, L., and Muller, R. N. (2008) Magnetic iron oxide nanoparticles: synthesis, stabilization, vectorization, physicochemical characterizations, and biological applications. *Chem. Rev. 108*, 2064−2110.
(43) Roch, A., Muller, R. N., and Gillis, P. (1999) Theory of proton relaxation induced by superparamagnetic particles. *J. Chem. Phys. 110*, 5403−5411.
(44) Boutry, S., Brunin, S., Mahieu, I., Laurent, S., Elst, L. V., and Muller, R. N. (2008) Magnetic labeling of non-phagocytic adherent cells with iron oxide nanoparticles: a comprehensive study. *Contrast Media Mol. Imaging 3*, 223−232.

DOI: 10.1021/acs.bioconjchem.5b00041
Bioconjugate Chem. 2015, 26, 822−829